The Heavy-Flavour Contribution to Proton Structure

K. Daum[a,b], S. Riemersma[c], B.W. Harris[d], E. Laenen[e], J. Smith[b,f]

[a] Rechenzentrum, Universität Wuppertal, Gaußstraße 20, D-42097 Wuppertal, Germany
[b] DESY, Notkestrasse 85, D-22603 Hamburg, Germany
[c] DESY-Zeuthen, Platanenallee 6 D-15738 Zeuthen, Germany
[d] Department of Physics, Florida State University, Tallahassee, Florida, 32306-3016, USA
[e] CERN Theory Division, CH-1211 Geneva 23, Switzerland
[f] Institute for Theoretical Physics, SUNY Stony Brook, NY 11794-3840, USA

Abstract: We present theoretical and experimental considerations pertaining to deeply inelastic heavy-flavour production. The various theoretical uncertainties in the cross section calculation are discussed. Cuts are imposed to determine the fraction of charm production accessible to the detectors. The production of charm at asymptotic Q^2 and bottom production are also covered. Experimental aspects include current charm production data analysis and prospects for future analyses including anticipated high precision and distinguishing photon-gluon fusion charm events from excitation from the charm parton density. The feasibility of measuring $F_2^{b\bar{b}}(x, Q^2)$ is investigated.

1 Introduction

Heavy-flavour production in deeply inelastic scattering (DIS) at HERA is now emerging as a very important means of studying proton structure. The ink is still drying on the first experimental reports of charm production from photon-mediated DIS at HERA [1, 2]. The next-to-leading order (NLO) calculations have also been published within the last four years. The inclusive calculation of the photon-mediated heavy-flavour structure functions $F_{2,L}^{\mathrm{hq}}(x, Q^2, m^2)$ [3], the inclusive single differential distribution $dF_{2,L}^{\mathrm{hq}}/dO$ [4] (O being the transverse momentum p_t of the heavy quark and the rapidity y), and the fully differential calculation [5] are now available for a complete NLO analysis of the photon-mediated heavy-flavour structure function.

In section 2, following a short review of the necessary formulae, we give event numbers for charm and bottom in bins of x and Q^2 and investigate the theoretical issues surrounding DIS heavy-flavour production. The primary sources of theoretical uncertainty include the imprecisely determined charm quark mass and renormalization and factorization scale dependences. Additional impediments to a clean extraction of the gluon density from heavy-flavour production include the effects of light-quark (u, d, s) initiated heavy-flavour production and the influence of the longitudinal heavy-flavour structure function $F_L^{\mathrm{hq}}(x, Q^2, m^2)$ upon the cross section results.

We investigate the effect of realistic cuts in p_t and pseudorapidity η on the cross section and determine acceptance probabilities as a function of x and Q^2. Charm production in the limit $Q^2 \gg m_c^2$ [6] is then discussed.

In section 3, we briefly summarize the analyses of charm production of the 1994 HERA data. These data allow for the determination of the source of the charm production, revealing the primary production mechanism at presently measured Q^2 values is photon-gluon fusion rather than stemming from the charm parton density. From the first measurement of the charm structure function $F_2^{c\bar{c}}$ at low x, the ratio $F_2^{c\bar{c}}/F_2$ is extracted.

Subsequently future experimental prospects are discussed. The current installation of the silicon vertex detectors at H1 will enable greater charm and bottom hadron detection efficiency. The anticipated luminosity of $500\,pb^{-1}$ will allow detailed studies of charm production dynamics. The transition from boson-gluon fusion of charm to excitation from the charm quark sea should become apparent as the accessible Q^2 grows. The predicted bottom quark production cross section will enable studies of $F_2^{b\bar{b}}/F_2^{c\bar{c}}$ as a function of x and Q^2 with reasonable precision.

2 Theoretical Aspects

2.1 Background

The reaction under study is

$$e^-(l) + P(p) \to e^-(l') + Q(p_1)(\bar{Q}(p_1)) + X\,, \tag{1}$$

where $P(p)$ is a proton with momentum p, $Q(p_1)(\bar{Q}(p_1))$ is a heavy (anti)-quark with momentum p_1 ($p_1^2 = m^2$) and X is any hadronic state allowed by quantum number conservation. The cross section may be expressed as

$$\frac{d^2\sigma}{dx\,dQ^2} = \frac{2\pi\alpha^2}{x\,Q^4}\left[(1+(1-y)^2)F_2^{\rm hq}(x,Q^2,m^2) - y^2 F_L^{\rm hq}(x,Q^2,m^2)\right]. \tag{2}$$

The inclusive structure functions $F_{2,L}^{\rm hq}$ were calculated to next-to-leading order (NLO) in Ref. [3]. The results can be written as

$$\begin{aligned} F_k(x,Q^2,m^2) &= \frac{Q^2\alpha_s(\mu^2)}{4\pi^2 m^2}\int_x^{z_{\max}}\frac{dz}{z}\Big[\,e_H^2 f_g(\frac{x}{z},\mu^2)c_{k,g}^{(0)}\Big] \\ &+ \frac{Q^2\alpha_s^2(\mu^2)}{\pi m^2}\int_x^{z_{\max}}\frac{dz}{z}\Big\{\,e_H^2 f_g(\frac{x}{z},\mu^2)(c_{k,g}^{(1)} + \bar{c}_{k,g}^{(1)}\ln\frac{\mu^2}{m^2}) \\ &+ \sum_{i=q,\bar{q}}\Big[e_H^2\, f_i(\frac{x}{z},\mu^2)(c_{k,i}^{(1)} + \bar{c}_{k,i}^{(1)}\ln\frac{\mu^2}{m^2}) + e_{L,i}^2\, f_i(\frac{x}{z},\mu^2)d_{k,i}^{(1)}\Big]\Big\}, \end{aligned} \tag{3}$$

where $k = 2, L$ and the upper boundary on the integration is given by $z_{\max} = Q^2/(Q^2+4m^2)$. The functions $f_i(x,\mu^2)\,,(i = g,q,\bar{q})$ denote the parton densities in the proton and μ stands for the mass factorization scale which has been set equal to the renormalization scale. The $c_{k,i}^{(l)}(\zeta,\xi)\,(i = g\,,q\,,\bar{q}\,;l = 0,1)$, $\bar{c}_{k,i}^{(l)}(\zeta,\xi)\,(i = g,q,\bar{q};l = 1)$, and $d_{k,i}^{(l)}(\zeta,\xi)\,(i = q\,,\bar{q}\,;l = 1)$ are coefficient functions and are represented in the $\overline{\rm MS}$ scheme. They depend on the scaling variables ζ and ξ defined by

$$\zeta = \frac{s}{4m^2} - 1 \qquad \xi = \frac{Q^2}{m^2}\,. \tag{4}$$

where s is the square of the c.m. energy of the virtual photon-parton subprocess $Q^2(1-z)/z$. In Eq. (3) we distinguish between the coefficient functions with respect to their origin. The coefficient functions indicated by $c_{k,i}^{(l)}(\zeta,\xi), \bar{c}_{k,i}^{(l)}(\zeta,\xi)$ originate from the partonic subprocesses where the virtual photon is coupled to the heavy quark, whereas $d_{k,i}^{(l)}(\zeta,\xi)$ comes from the subprocess where the virtual photon interacts with the light quark. The former are multiplied by the charge squared of the heavy quark e_H^2, and the latter by the charge squared of the light quark e_L^2 respectively (both in units of e). Terms proportional to $e_H e_L$ integrate to zero for the inclusive structure functions. Furthermore we have isolated the factorization scale dependent logarithm $\ln(\mu^2/m^2)$.

We investigate the ability of heavy-flavour production to constrain the gluon density. The scale dependence and the poorly known charm quark mass are the largest contributors to the theoretical uncertainty. The effects of F_L^{hq} and the light-quark initiated contributions are discovered also to be important in the analysis. To aid the experimental analysis, the fully differential program [5] is used to apply a series of cuts to determine the percentage of events the detectors are likely to see in bins of x and Q^2. With the planned inclusion of silicon vertex detectors, the ability to see bottom events increases dramatically, motivating the presentation of results for the cross section and $F_2^{b\bar{b}}(x,Q^2,m_b^2)$. The transition of charm production from photon-gluon fusion to excitation from the charm parton density is something HERA is in a unique position to evaluate. For other phenomenological investigations, see [8, 9, 10].

2.2 Code Update

For this study we use an updated version of the code based upon [7]. The original code was based upon fitting the coefficient functions described in eq. (3) using a two-dimensional tabular array of points in ζ and ξ. The coefficient functions were generated via a linear interpolation between the calculated points. The linear interpolation was insufficiently accurate and required a more sophisticated interpolation procedure.

The present interpolation procedure is based upon a Lagrange three-point interpolation formula, see eq. 25.2.11 [11]. The results have been thoroughly compared with the original code in [3] and [5] and excellent agreement has been established.[1]

As a demonstration of the code, we present results for the Born $c_2^{(0)}(\zeta,\xi=1,10)$ in Fig. 1a and $c_{2,g}^{(1)}(\zeta,\xi=1,10)$ and $\bar{c}_{2,g}^{(1)}(\zeta,\xi=1,10)$ in Fig. 1b.

2.3 Scale and Parton Density Related Issues

For the subsequent studies we first construct a "data" set. The number of DIS charm events is calculated for an integrated luminosity of $500\,pb^{-1}$, using CTEQ3M [12] parton densities with $\Lambda_4 = 239$ MeV, $m_c = 1.5$ GeV, and $\mu^2 = Q^2 + 4\,m_c^2$. Unless otherwise mentioned, CTEQ3M is used for all results. The results in Fig. 2a. are produced for $1.8 < Q^2 < 1000$ GeV^2 and $10^{-4} < x < 1$ using four bins per decade for both Q^2 and x.

We also calculate the amount of bottom production events, which is greatly reduced due to the reduction of the charge factor by four as well as a significantly reduced phase space. The

[1] The code is available at http://www.ifh.de/theory/publist.html.

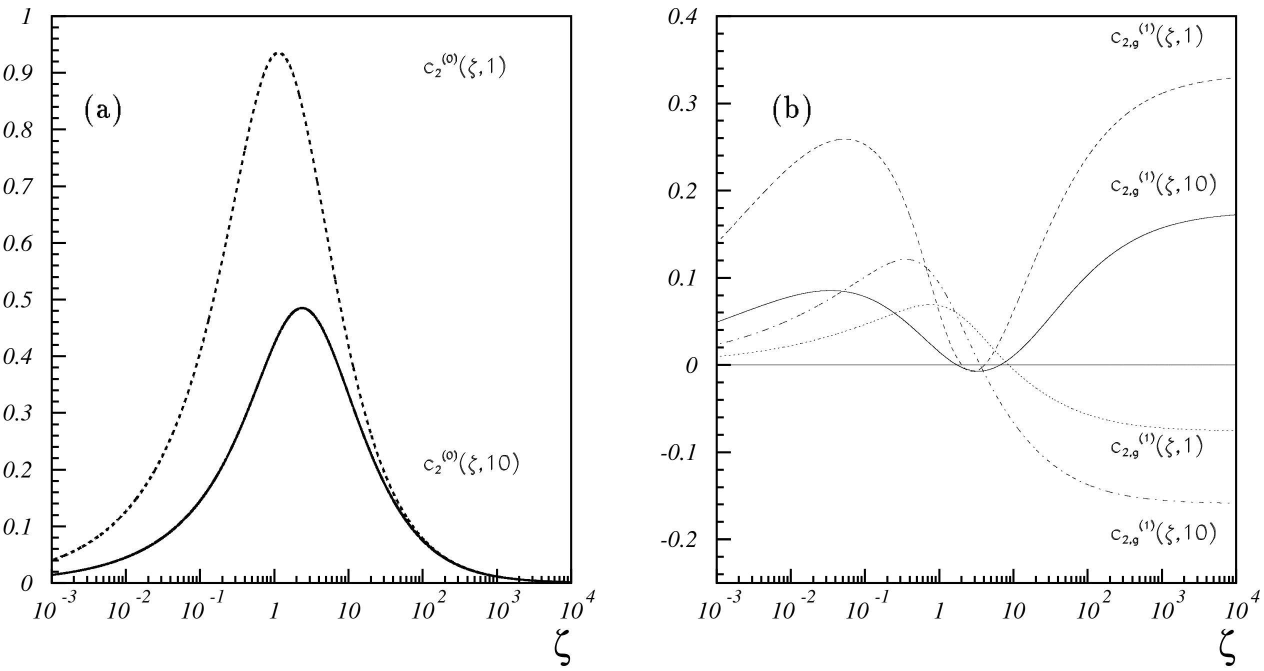

Figure 1: *(a) The Born coefficient function $c_2^{(0)}(\zeta,\xi)$, for $\xi = 1, 10$ and (b)The NLO coefficient functions $c_{2,g}^{(1)}(\zeta,\xi)$, for $\xi = 1, 10$ (upper curves at large ζ) and $\bar{c}_{2,g}^{(1)}(\zeta,\xi)$ for $\xi = 1, 10$ (lower curves at large ζ).*

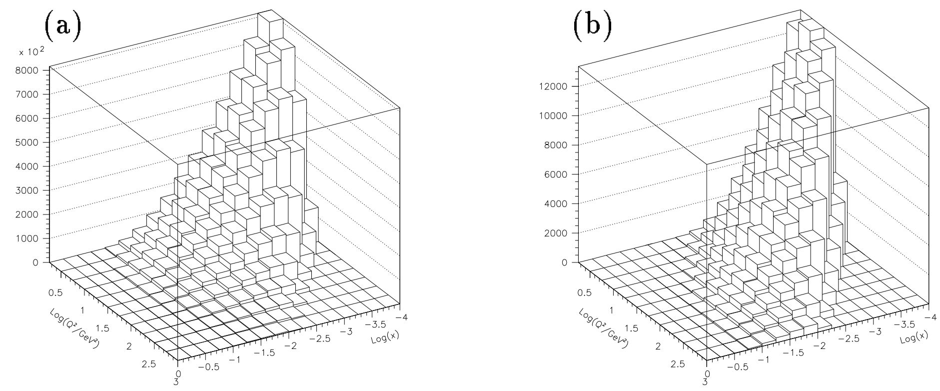

Figure 2: *Projected number of DIS events from (a) charm and (b) bottom production for an integrated luminosity of 500 pb^{-1} binned in x and Q^2 with no cuts applied.*

result is shown in Fig. 2b taking the same parameters as before except $m_b = 4.75$ GeV and $\mu^2 = Q^2 + m_b^2$. A discussion of the implications of this number of b events can be found in section 3.2.

The most important numerical sources of theoretical uncertainty in DIS heavy-flavour production are the factorization/renormalization scale dependence and the poorly known charm quark mass. Varying μ in Eq. (3) indicates the stability of the NLO result is against scale changes.

The "data" are peaked strongly at small x and Q^2. As Q^2 grows, the events become more evenly distributed in x. For small Q^2, the number of events N falls off as $x \to 1$. At larger Q^2, N rises, peaks at intermediate x, then drops.

Using the "data" set as a point of reference, we can investigate where in the kinematic region the effects of scale variation are most strongly felt. Keeping every other parameter fixed,

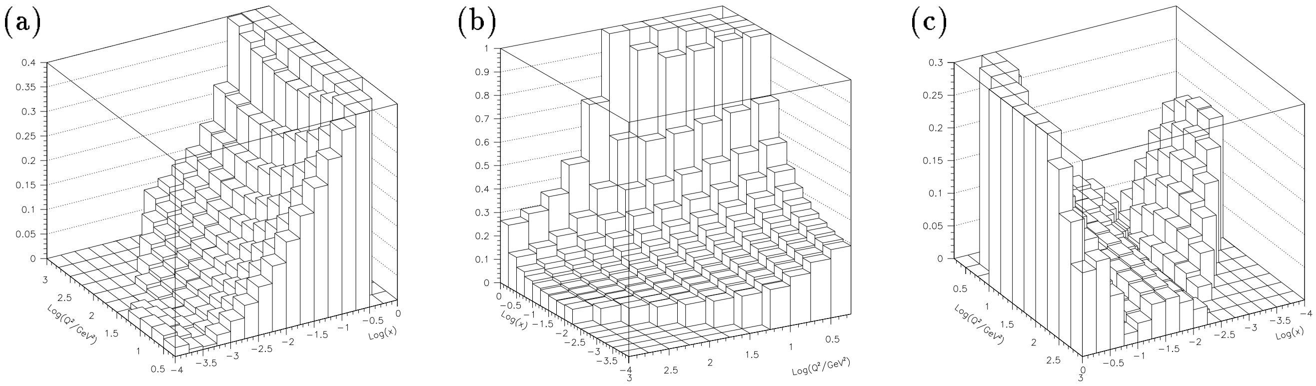

Figure 3: *The uncertainties in $\sigma(ep \to c\bar{c}X)(x,Q^2)$: (a) Δ_μ,(b) Δ_{m_c}, and (c) $\Delta_{\rm glue}$.*

we determine the number of events for $\mu^2 = 4m_c^2$ and $\mu^2 = 4(Q^2 + 4m_c^2)$. We investigate the quantity

$$\Delta_\mu(x,Q^2) \equiv \left|\frac{N(\mu^2 = 4m_c^2) - N(\mu^2 = 4(Q^2+4m_c^2))}{2N(\mu^2 = Q^2 + 4m_c^2)}\right|. \tag{5}$$

The results are displayed in Fig. 3a. Apart from the high-x region, which contains very few charm events, the scale dependence varies relatively little with Q^2. As $x \to 0$, we find the scale dependence disappearing. This behaviour bodes very well for a low-x extraction of the gluon density from charm events.

The charm quark mass uncertainty presents a stickier problem. A precise measurement of the charm mass is yet to be made. To develop a feeling for how much of an effect the uncertainty has, we calculated

$$\Delta_{m_c}(x,Q^2) \equiv \frac{N(m_c = 1.3\mathrm{GeV}) - N(m_c = 1.7\mathrm{GeV})}{2\,N(m_c = 1.5\mathrm{GeV})}. \tag{6}$$

Very large effects are naturally found near threshould, but as Q^2 increases and x decreases, Δ_{m_c} approaches a value on the order of 0.1. Varying the charm mass from 1.3 to 1.7 GeV is a conservative estimate; the error induced by the uncertainty viewed in Fig. 3b. can be viewed as an upper bound.

A clear indication of the ability to extract the gluon density from charm production is whether one can distinguish the gluon densities from different available parton densities. We compare the cross section generated with CTEQ2MF[12] (with a flat gluon density as $x \to 0$) with GRV94HO[13] (with a steep gluon density as $x \to 0$). We define

$$\Delta_{\rm glue}(x,Q^2) \equiv \left|\frac{N_{\rm CTEQ2MF} - N_{\rm GRV94HO}}{2\,N_{\rm CTEQ3M}}\right| \tag{7}$$

and show the results in Fig. 3c.

Away from large x, $\Delta_{\rm glue}(x,Q^2)$ is flat as a function of Q^2. In the intermediate region in x, very little distinguishing power is observed. Beginning near $x = 10^{-3}$, a definite difference is seen. The analysis must seemingly extend to $x \lesssim 5 \cdot 10^{-4}$ to distinguish cleanly the gluon densities mentioned.

To summarize: While the scale dependence is well under control, the dominant source of uncertainty is clearly the charm quark mass, which has a strong influence on the cross section at low x and low Q^2. This region is exactly the region sensitive to the gluon density. This strong influence of m_c poses problems for a clean extraction of the gluon density at small x from inclusive measurements.

2.4 Smaller Contributions to the Cross Section: $F_L^{c\bar{c}}$ and Light-Quark Initiated Results

A clean extraction of the gluon density may be hindered by contributions of $F_L^{c\bar{c}}$ and light-quark initiated contributions to the cross section. We investigate the fractional F_L contribution to the cross section by investigating

$$C_{F_L} \equiv \left| \frac{\sigma_{tot} - \sigma_{F_2}}{\sigma_{tot}} \right|, \tag{8}$$

where σ_{F_2} represents the contribution to the cross section in Eq. (2) with F_L set to zero.

We find a sizeable contribution to the cross section at high y. This overlaps with the low Q^2 and low x region previously determined to be deemed the most suitable for a gluon density extraction. To do so, however, one must take into consideration $F_L^{c\bar{c}}$.

We investigate the light-quark initiated contribution by determining

$$C_{\mathrm{lq}} = \left| \frac{\sigma_{\mathrm{lq}}}{\sigma_{tot}} \right|. \tag{9}$$

The results are very nearly constant, amounting to a 5 – 8 % contribution except at large x, where the charm contribution does not appreciably contribute numerically.

Summarizing: the contributions to the cross section from $F_L^{c\bar{c}}$ are noticeable in the large y region, which overlaps with the small x and small Q^2 region, hindering the extraction of the gluon using only $F_2^{c\bar{c}}$. The light-quark initiated cross section contributes on the order of 5 % to the total cross section, and therefore cannot be totally neglected.

2.5 Cuts *vs.* No Cuts

With the fully differential code developed in [5], a series of cuts can be applied determining a more realistic expectation of charm events able to be detected.

The cuts imposed upon the data are

$$|\eta_c| \leq 1.5, \; p_t^c \geq 2\,\mathrm{GeV}, \tag{10}$$

η_c being the pseudorapidity of the detected charm quark. We define the efficiency as the percentage of the cross section surviving the cuts relative to the the uncut cross section. Looking first at the low Q^2 range from 2 to 10 GeV^2 (σ_L), we present the cross section with and without the aforementioned cuts in the x bins outlined in Tab. 1. In the low x range, we observe an efficiency of 20 – 25 %, diminishing near threshould, the low efficiency mostly a result of the p_t cut.

In the intermediate Q^2 range (σ_I), from 10 to 100 GeV^2. We find the efficiency has risen considerably to the 30–40 % range where the cross section is peaked in intermediate x, with on the order of 20 % for the small x region.

In the high Q^2 range, from 100 to 1000 GeV^2 (σ_H), the efficiency continues to rise with Q^2, reaching 50–60 % in the high to intermediate x region and 30–40 % in the small x range.

The number of events falling within the imposed cuts mentioned in Eq. (10) is not overwhelmingly large, but a large enough sample should be accessible to gather significant statistics.

x_{min}	x_{max}	σ_L (nb)	$\sigma_{L,cuts}$ (nb)	σ_I (nb)	$\sigma_{I,cuts}$ (nb)	σ_H (nb)	$\sigma_{H,cuts}$ (nb)
0.10E-3	0.18E-3	4.39	1.06	0.33	0.06		
0.18E-3	0.32E-3	4.14	1.13	1.16	0.25		
0.32E-3	0.56E-3	3.60	0.96	1.73	0.48		
0.56E-3	0.10E-2	2.96	0.70	1.98	0.68		
0.10E-2	0.18E-2	2.32	0.40	1.91	0.77	0.040	0.012
0.18E-2	0.32E-2	1.74	0.17	1.62	0.70	0.12	0.049
0.32E-2	0.56E-2	1.25	0.04	1.27	0.50	0.16	0.089
0.56E-2	0.10E-1	0.85	0.002	0.94	0.28	0.16	0.096
0.10E-1	0.18E-1			0.66	0.11	0.13	0.076
0.018	0.32E-1			0.43	0.025	0.091	0.046
0.032	0.56E-1			0.26	0.014	0.057	0.017
0.56E-1	0.10E+0			0.13	0.000	0.032	0.003
0.10E+0	0.18E+0					0.014	0.000
0.18E+0	0.32E+0					0.041	0.000

Table 1: *Cross sections with and without the cuts mentioned in Eq. (10).*

2.6 Charm Production at Asymptotic Q^2

Near the threshould for charm production the deep inelastic structure functions F_i, $i = 2, L$, which include the contributions of the light partons u, d, s, and g and the charm quark with mass m_c are given by eq. (3).

Equation (3) gives an adequate prescription as long as the c.m. energy is not too far above the charm threshould, which implies that Q^2 is not too large compared to m_c^2. However, when we enter the asymptotic region $Q^2 \gg m_c^2$, the heavy quark coefficient functions behave like $\ln^i(m_c^2/\mu^2)\ln^j(Q^2/m_c^2)$ so that the higher order corrections can become large. At sufficiently large Q^2 the charm quark should be treated in the same way as the light partons were at smaller Q^2. The logarithmic behaviour of the coefficient functions is due to the collinear singularities which are regulated by m_c. Therefore when $Q^2 \gg m_c^2$, the charm quark behaves like a massless quark similar to the behaviour of the normal light quarks (u, d, and s) over the whole Q^2 range. Following the same procedure as has been used for the light partons, the mass singular (m_c -dependent) terms have to be factorized out of the heavy quark coefficient functions using the method of mass factorization. This leads to a redefinition of the parton densities and the heavy quark coefficient functions turn into the light parton analogues, wherein the number of light flavours is enhanced by one. The above procedure is called the variable flavour number scheme (VFNS) which is outlined in leading order in [14].

Since all coefficient functions are now available up to order α_s^2, this analysis can be extended to NLO to give a better description for the structure functions $F_i(x, Q^2)$ at large Q^2. A preprint is in preparation[15].

3 Experimental Aspects

3.1 Charm production

Results on charm production in deep inelastic ep scattering are available H1 and ZEUS based on a luminosity of approximately 3 pb^{-1} collected with each experiment at HERA in 1994. The H1 collaboration [1] has performed the tagging of heavy quark events by reconstructing $D^0/\overline{D}^0(1864)$ and $D^{*\pm}(2010)$ mesons, while the ZEUS collaboration [2] has given preliminary results for the inclusive $D^{*\pm}(2010)$ analysis. The number of currently observed events containing heavy quarks is only of the order of 100 to 200 charm mesons identified in any of the different analyses. Combining the D^0 and $D^{*\pm}$ analysis of H1 leads to a charm production cross section of

$$\sigma(ep \to ec\bar{c}X) = 17.4 \pm 1.6(\mathit{stat.}) \pm 1.7(\mathit{exp.syst.}) \pm 1.4(\mathit{model})\ \mathrm{nb} \tag{11}$$

in the kinematic range 10 GeV^2 $<$ Q^2 $<$ 100 GeV^2 and $0.01 < y < 0.7$. This cross section is somewhat larger than predicted by the NLO calculations [3, 1].

H1 has also extracted information on the charm production mechanism in neutral current DIS at HERA from the distribution of $x_D = 2|\vec{P}^*_{D^0}|/W$, where $\vec{P}^*_{D^0}$ denotes the momentum of the D^0 in the $\gamma^* p$ system. This is found to agree well with the expectation from boson gluon fusion, but disagrees with the prediction from processes in which the charmed hadrons would originate directly from quarks in the proton. This analysis concludes that over 95% of charm production in neutral current ep DIS is due to boson-gluon fusion. This observation seems to be in contradiction to recent inclusive calculations of charm production in DIS [14], from which was concluded that for the kinematic range accessible in the current analyses at HERA charm quarks may already be considered as partons in the proton [10].

Finally, current charm production data allowes for a first glimpse at the charm contribution $F_2^{c\bar{c}}(x, Q^2)$ to the proton structure function at small x. Although the errors on the indivial data points are still large ($\mathcal{O}(20 - 30\%)$), clearly the charm contribution is important. Averaged over the kinematic range, a ratio $\left\langle F_2^{c\bar{c}}/F_2 \right\rangle = 0.237 \pm 0.021 \pm 0.041$ is obtained, which is one order of magnitude larger than at larger x.

In the following we give some estimates about the precision that may be expected at HERA for an integrated luminosity of 500 pb^{-1}. As an example the capabilities of the H1 detector [18] are considered. For heavy flavor physics an important new feature of the apparatus is the double layer silicon vertex detector (CST) [19] which will allow use of the apparent proper time of charm hadrons in selecting heavy flavor events. Other decay channels than $D^0 \to K^-\pi^+$ and $D^{*+} \to D^0\pi_s^+ \to K^-\pi^+\pi_s^+$ are already under investigation or will become accessible due to the CST.

Table 2 contains a list of decay modes which should be feasible for charm tagging in H1 in future by also including the CST. A total charm selection efficiency of 1% may be obtained. Compared to the present analysis this corresponds to an increase in the total selection efficiency of a factor 4 to 5. Although the new channels opened by the use of the CST corresponds only to 50% of this gain, the signal to background ratio will improve for all decay modes considerably. From the improved signal to background ratio, the improved effective number of events per luminosity $N_{eff} = (N_{signal}/\sigma_{stat})^2$ will increase by a factor of 6 to 8. Due to the cut in the impact parameter of the D^0 mesons, which is likely to be different in the D^0 and D^{*+} analyses, the events selected in the D^{*+} analyses will only partially overlap with the events selected in

Mode		$P(c \to D)$	$BR(D \to FS)$	ϵ_{tot}	$P \cdot BR \cdot \epsilon_{tot}$
$D^{*+} \to D^0\pi_s^+ \to K^-\pi^+\pi_s^+$	[1]	0.248	0.026	0.16	0.0010
$D^{*+} \to D^0\pi_s^+ \to K^-\pi^+\pi^0\pi_s^+$			0.096	0.04	0.0010
$D^{*+} \to D^0\pi_s^+ \to K^-3\pi\pi_s^+$			0.052	0.10	0.0013
$D^{*+} \to D^0\pi_s^+ \to K^0\pi^+\pi^-\pi_s^+$			0.013	0.20	0.0007
$D^{*+} \to D^0\pi_s^+ \to K^0\pi^+\pi^-\pi^0\pi_s^+$			0.024	0.08	0.0005
$D^{*+} \to D^0\pi_s^+ \to K^-\mu^+\nu_\mu\pi_s^+$			0.024	0.04	0.0002
$D^{*+} \to D^0\pi_s^+ \to K^-e^+\nu_e\pi_s^+$			0.024	0.04	0.0002
Sum D^{*+}		0.248	0.259		0.0049
$D^0 \to K^-\pi^+$	[1]	0.535	0.0383	0.06	0.0012
$D^0 \to K^0\pi^+\pi^-$			0.0186	0.06	0.0006
$D^0 \to K^-3\pi$	CST		0.075	0.04	0.0014
Sum D^0		0.535	0.132		0.0032
$D^+ \to K^0\pi^+$	CST	0.25	0.009	0.12	0.0003
$D^+ \to K^-\pi^+\pi^-$	CST		0.091	0.07	0.0016
$D^+ \to K^03\pi$	CST		0.07	0.07	0.0012
Sum D^+	CST	0.25	0.170		0.0031
Sum D					0.0097

Table 2: *Compilation of various decay channels of charm mesons accessible in H1. The channels marked by "CST" will be accessible only by using the silicon vertex detector. $BR(D \to FS)$ denotes the product of all branching ratios involved in the decay into the final state "FS". For the determination of the total charm tagging efficiency the correlations in the D^0 and D^{*+} analyses are taken into account.*

the corresponding D^0 analyses. Taking an integrated luminosity of 500 pb^{-1}, about 160,000 tagged charm events are expected for the kinematic range of the published H1 analysis. This has to be compared to the currently analyzed 250 events. We expect a gain of a factor of 1000 is expected for the statistical significance because of the increase in the effective number of events. In total, we expect to observe roughly 6,000 double-tag charm events in the range 1.7 GeV$^2 < Q^2 <$ 560 GeV^2 which would allow a study of the charm production dynamics in detail (see Ref. [10]).

Figure 4 shows the result of the hypothetical measurement of $F_2^{c\bar{c}}$ in the range 1.7 GeV$^2 < Q^2 <$ 560 GeV^2 for a luminosity of 500 pb^{-1} based on the gluon density determination from the NLO H1 fit to the inclusive F_2 data combining the statistics of the D meson decay modes summarized in Table 2 by assuming $m_c = 1.5$ GeV and $\mu^2 = Q^2 + 4m_c^2$. The contribution due to F_L and the light flavors are not included. Statistical and full errors are shown. The effect due to the uncertainty in m_c and μ is not included. For $Q^2 <$ 100 GeV^2 the precision of this measurement will be limited by the experimental systematic uncertainty.

A detailed analysis of the experimental systematic uncertainties in the determination of $F_2^{c\bar{c}}$ based on the current data is given in Ref. [1]. At present the total systematic error is approximately 20 %. It is dominated by the uncertainty in the assumptions made to extract the signal from the observed mass distributions. This will improve as soon as more data become available. Ultimately a systematic error of 10% is achievable, which will then be equally due to

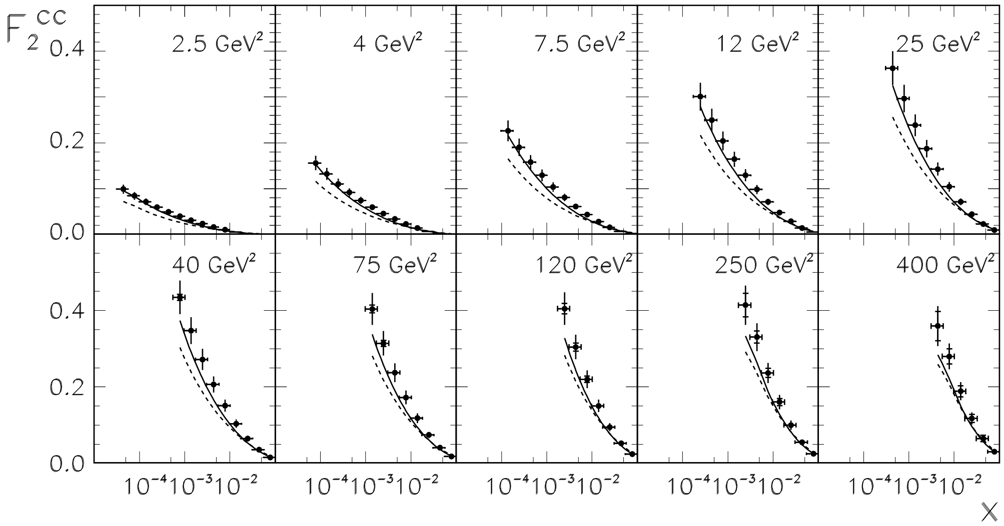

Figure 4: *Expected $F_2^{c\bar{c}}$ for a luminosity of 500 pb^{-1}. The points show the prediction from the gluon density determination by the NLO H1 fit to the inclusive F_2. The inner (outer) error represents the statistical and the total experimental error. The full (dashed) line gives the expectation from the NLO calculations based on GRV-HO [16] and MRSH [17] parton distributions using a charm quark mass of $m_c = 1.5$ GeV.*

detector and analysis related errors (7%) and to the knowledge of the fragmentation probability $P(c \rightarrow D)$ of a charm quark into a specific charm meson and their branching ratios (7%). The latter will not improve in the near future.

Figure 4 also shows the NLO predictions [3, 7] using the GRV-HO(1992) [16] and the MRSH [17] parameterization of the gluon density in the proton using $m_c = 1.5$ GeV and $\mu^2 = Q^2 + 4m_c^2$. For a given value of m_c the data will still allow a sensitive indirect determination of the gluon density even with the relatively large experimental systematic uncertainties. Due to the high statistics it will be possible to measure the charm production cross section up to $Q^2 \leq 1000$ GeV^2. Assuming charm tagging is performed for all decay modes listed in Tab. 2, the sensitivity limit for the inclusive measurements will already be reached at 50 pb^{-1} for $Q^2 \leq 100$ GeV^2, at which time the experimental systematic will dominate in this kinematic range.

As shown in the theory section, the measurement of $F_2^{c\bar{c}}$ is sensitive to the gluon density at large y. Unfortunately the $F_2^{c\bar{c}}$ measurement in this range is also very sensitive to the charm quark mass. Therefore it is not clear whether the measurement of $F_2^{c\bar{c}}$ alone will allow an extraction of the gluon density at small x. For the present data [1] it was concluded that the extraction of the gluon density from $F_2^{c\bar{c}}$ should be still feasible. The behavior for $Q^2 < 10$ GeV^2 has not been studied yet. If it happens that $F_2^{c\bar{c}}$ does not provide an reliable indirect extraction of the gluon density because of the uncertainty in m_c, exclusive distributions of the identified charm hadrons have to be studied. As an example the result of the Monte Carlo study of the influence of m_c and the gluon density on the distribution $1/\sigma \ d\sigma/dx_D$ is shown in Fig. 5 for 6 GeV$^2 < Q^2 < 100$ GeV^2 and the cuts of Eq. (10). Here $\Delta \ x_D$ is defined as

$$\Delta \ x_D = \frac{1/\sigma_i \ d\sigma_i/dx_D(x_D)}{1/\sigma_j \ d\sigma_j/dx_D(x_D)} \tag{12}$$

where i, j denote the different values of the parameters, *i.e.* $m_c = 1.3$, 1.7 GeV and PDF=MRSH, GRV-HO(1992), respectively. The mass of the charm quark affects strongly

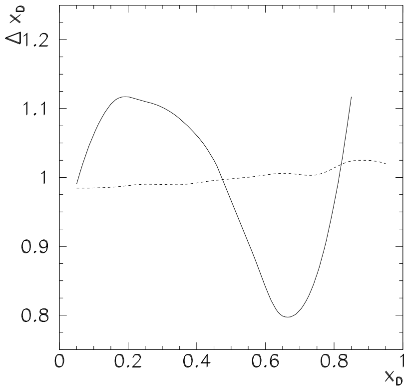

Figure 5: *Relative change Δx_D in the shape of the distribution $1/\sigma\ d\sigma/dx_D$ according to the LO Monte Carlo Simulation of the AROMA program for 6 $GeV^2 < Q^2 <$ 100 GeV^2 and the cuts of Eq. (10). The full line gives the change in the shape by changing m_c from* 1.3 *GeV to* 1.7 *GeV. The dashed line shows the influence of using the GRV-HO (1992) instead of the MRSH parameterization of the gluon density in the proton.*

the shape of the x_D distribution (full line) while there is only very little effect due to the choice of the parton density function (dashed line). A study of this distribution, for instance, should therefore disentangle the effect of the charm quark mass and the gluon density on $F_2^{c\bar{c}}$.

In section 2.5, the question when charm quarks should be treated as partons of the proton was discussed. The investigation of the x and Q^2 dependence of the exclusive measurement of $1/\sigma\ d\sigma/dx_D$ will allow a study of the origin of charm production as a function of the kinematic variables. At sufficiently large Q^2 it is expected that the charm quark behaves like a parton in the proton. This will result in a change of the x_D distribution from the boson gluon fusion dominated regime presently observed in the available data at $\langle Q^2 \rangle \approx 25$ GeV^2 to the sea quark dominated regime at large Q^2. If it becomes possible to control the μ and m_c dependence of charm production at large Q^2, the measurement of $F_2^{c\bar{c}}(x, Q^2, x_D)$ can determine $g(x, Q^2)$ and $c(x, Q^2)$ simultaneously. This study would certainly require a luminosity of 500 pb^{-1} to produce enough data at large Q^2.

3.2 Bottom Production

In the following the possibilities to measure $F_2^{b\bar{b}}(x, Q^2)$ at HERA are studied on the basis of the predictions for bottom production in section 2.3. Again the H1 detector is used as an example.

Compared to charm quark events the major experimental difference in bottom quark production is the relative long lifetime of the B mesons. With use of the CST, bottom events are selected by applying a cut in the impact parameter of tracks not fitting to the primary event vertex. The combinatorial background is negligible, while the charm production is a significant background source, because of the much larger cross section. Only the exclusive analysis of reconstructed D mesons will be discussed here. This method benefits from (a) the large branching ratios of B mesons into charm meson and (b) the relatively long visible lifetime observed in the decay chains. For a selection efficiency of 50% for the impact parameter cut, the contamination of charm events reduces by a factor of 12.5(2.8) for the $D^0(D^\pm)$ analysis.

All decay modes summarized in Tab. 2 will also be accessible in this case. Due to the larger cut values in the impact parameter for the different decay modes, the combinatorial background

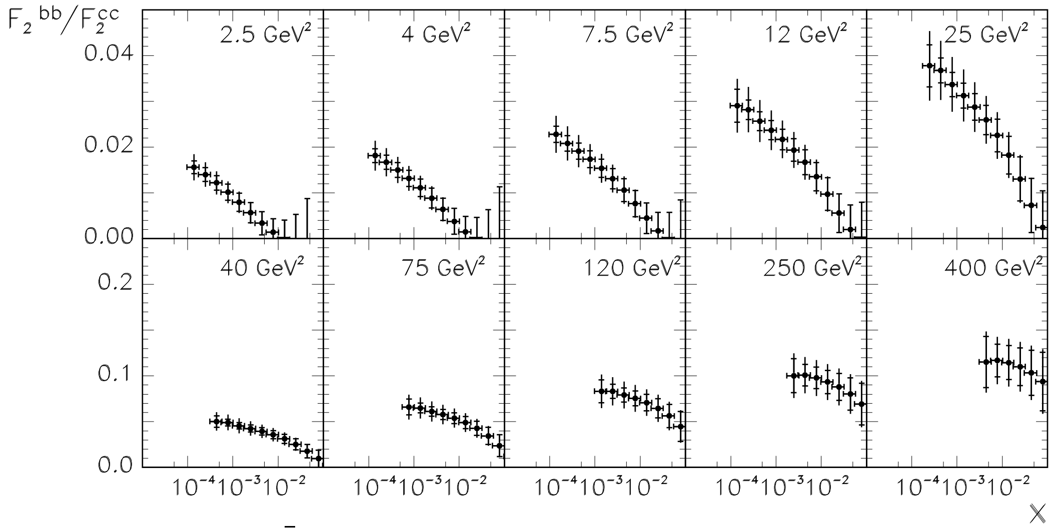

Figure 6: *Expected ratio $F_2^{b\bar{b}}/F_2^{c\bar{c}}$ for a luminosity of 500 pb^{-1}. The points show the predictions according to the calculations of section 2.1 and 2.6. The inner (outer) error represents the statistical and the total experimental error.*

is smaller. This will allow for softer cuts. Compared to charm production studies an increase in efficiency by a factor 3 is expected. A systematic error of 16% may be achieved, limited by the uncertainties in the branching fraction $BR(B \to DX)$.

Figure 6 shows the ratio of $F_2^{b\bar{b}}/F_2^{c\bar{c}}$ expected from this analysis where the charm production background is subtracted statistically. The errors refer to the statistical and the total experimental error. For a luminosity of 500 pb^{-1} will still be statistics limited. Integrated over the kinematic range a mean value of $F_2^{b\bar{b}}/F_2^{c\bar{c}} \approx 0.02$ is predicted.

4 Conclusions

In this paper, we have discussed DIS heavy-flavour production at HERA at NLO. The effect on the charm production cross section due to the uncertainties in the factorization/renormalization scale μ and the charm quark mass m_c has been studied as a function of x and Q^2. At small x and for $Q^2 < 300$ GeV^2 the predictions are found to be insensitive to μ while in this region the effect of m_c is found to be large. Unfortunately the sensitivity of $F_2^{c\bar{c}}(x, Q^2)$ to the gluon density at small x is also restricted to this kinematic region. It has been shown that the contribution of F_L has sizeable effects on the charm production cross section at large y. The contribution of light quarks to the cross section turned out to be of the order of 5%, nearly independent of x and Q^2. Results on bottom production have been presented.

The current experimental situation has been summarized. Based upon this knowledge, statistical and experimental systematic uncertainties for large luminosity have been estimated. Ultimately an accuracy of 10% in the overall normalization of the cross section may be achieved. In the kinematic range where the inclusive measurement $F_2^{c\bar{c}}(x, Q^2)$ is found to be sensitive to the gluon density, the error of the inclusive measurement will start to be systematics dominated with a luminosity of 50 pb^{-1}. It has been demonstrated that exclusive measurements of the charm mesons would disentangle the influence of m_c and the gluon density on the charm production cross section. An exploration of the kinematic plane, the extraction of the gluon density, as well as the question when the charm quark may be treated as a parton, will require a luminosity of 500 pb^{-1}. Finally the ratio of $F_2^{b\bar{b}}/F_2^{c\bar{c}}(x, Q^2)$ has been investigated by performing an exclusive D meson analysis. With a luminosity of 500 pb^{-1} the predicted statistics is found to be sufficient to make a detailed study of the x and Q^2 dependence of this ratio.

Acknowledgments

S.R. thanks Jenny Ivarsson for her help making the figures.

References

[1] C. Adloff *et al.*, H1 Collaboration, DESY 96-138, accepted by Z. Phys. **C** (1996).

[2] ZEUS Collaboration, contributed paper to XXVIII Int. Conf. on HEP '96, Warsaw (1996).

[3] E. Laenen, S. Riemersma, J. Smith, and W.L. van Neerven, Nucl. Phys. **B392** (1993) 162.

[4] E. Laenen, S. Riemersma, J. Smith, and W.L. van Neerven, Nucl. Phys. **B392** (1993) 229.

[5] B.W. Harris and J. Smith, Nucl. Phys. **B452** (1995) 109; Phys. Lett. **353B** (1995) 535; B.W. Harris, talk A05057, presented at the American Physical Society, Division of Particles and Fields 1996 Meeting, Minneapolis, Minnesota, 10-15 August 1996, to appear in proceedings.

[6] M. Buza, Y. Matiounine, R. Migneron, J. Smith, and W.L. van Neerven, Nucl. Phys. **B472** (1996) 611.

[7] S. Riemersma, J. Smith, and W.L. van Neerven, Phys. Lett. **347B** (1995) 143.

[8] E. Laenen, S. Riemersma, J. Smith, and W.L. van Neerven, Phys. Letts. **291B** (1992) 325.

[9] A. Vogt, DESY 96-012, hep-ph/9601352

[10] E. Laenen, M. Buza, B.W. Harris, Y. Matiounine, R. Migneron, S. Riemersma, J. Smith, and W.L. van Neerven, these proceedings.

[11] Handbook of Mathematical Functions, eds. M. Abramowitz and I.E. Stegun, National Bureau of Standards, (1972) 879.

[12] H.L. Lai, J. Botts, J. Huston, J.G. Morfin, J.F. Owen, J.W. Qiu, W.K. Tung, and H. Weerts, Phys. Rev. **D51** (1995) 4763.

[13] M. Glück, E. Reya, and A. Vogt, Z. Phys. **C67** (1995) 433.

[14] M.A.G. Aivazis, F.I. Olness, and W-K. Tung, Phys. Rev. **D50** (1994) 3085; M.A.G. Aivazis, J.C. Collins, F.I. Olness, and W-K. Tung, Phys. Rev. **D50** (1994) 3102.

[15] M. Buza, Y. Matiounine, J. Smith and W.L. van Neerven, in preparation.

[16] M. Glück, E. Reya, and A. Vogt, Z. Phys. **C53** (1992) 127.

[17] P.N. Harriman, A.D. Martin, W.J. Stirling, and R.G. Roberts, Phys.Rev.**D42** (1990) 798.

[18] S. Aid et al., H1-Coll, DESY 96-01, accepted to Nucl. Inst. and Meth. (1996).

[19] W. Erdmann et al., Nucl. Inst. and Meth. **A372** (1996) 188.